Numer. Math. (2001) 90: 241–264
Digital Object Identifier (DOI) 10.1007/s002110100303

Numerische Mathematik

Heterogeneous coupling by virtual control methods

P. Gervasio[1], **J.-L. Lions**[2], **A. Quarteroni**[3,4]

[1] Department of Mathematics, University of Brescia, via Valotti 9, 25133 Brescia, Italy; e-mail: gervasio@ing.unibs.it
[2] Collège de France, 3, rue d'Ulm, 75231 Paris Cedex 05, France
[3] Department of Mathematics, EPFL, 1015 Lausanne, Switzerland
[4] Department of Mathematics, Politecnico di Milano, via Bonardi 9, 20133 Milano, Italy; e-mail: Alfio.Quarteroni@epfl.ch

Received October 2, 2000 / Published online May 30, 2001 –

Summary. The virtual control method, recently introduced to approximate elliptic and parabolic problems by overlapping domain decompositions (see [7–9]), is proposed here for heterogeneous problems. Precisely, we address the coupling of an advection equation with a diffusion-advection equation, with the aim of modelling boundary layers. We investigate both overlapping and non-overlapping (disjoint) subdomain decompositions. In the latter case, several cost functions are considered and a numerical assessment of our theoretical conclusions is carried out.

Mathematics Subject Classification (1991): 65N30, 65N55, 93C20

1. Introduction

Domain decomposition methods provide a well consolidated approach for an efficient solution of boundary-value problems. On one hand, they allow to devise parallel algorithms by reducing the original problem to a sequence of "independent" subproblems in smaller and simpler subdomain, see [3, 13, 12].

On the other hand, subdomain splitting is an interesting path towards multiphysics, i.e. the use of mathematical models based on different kind of partial differential equations to address physical problems of heterogeneous nature in different subregions of the given computational domains. This approach is given the name heterogeneous domain decomposition: for an introductory presentation see, e.g. [12, Ch. 8].

Correspondence to: A. Quarteroni

In the framework of advection-diffusion equations with boundary-layer solutions, heterogeneous domain decomposition methods, with disjoint subdomains, have been proposed and analyzed in [4, 5, 11].

In this article, heterogeneous methods for advection-diffusion equations are proposed in the context of virtual control-problems. Virtual control is a powerful technique that has been introduced in domain decomposition method with overlapping subdomains to treat "homogeneous" problems, either elliptic and parabolic (see [7–9]).

In this paper, virtual control is used to achieve interface continuity for both cases of overlapping or non overlapping (disjoint) subdomains. The discussion (and analysis) is carried out on the differential problem, however the theoretical conclusions that are drawn are assessed and verified at the finite dimensional level afterwards.

A particularly interesting corollary of our theory is that in the non overlapping case the results obtained in this paper, through minimization of a suitable cost functional, are coherent with those of [5] (and reported in [12, Ch. 8]), that were achieved by a singular perturbation theory.

This paper is organized as follows.

In Sect. 2 we set up the domain decomposition problem in the overlapping situation. In Sect. 3 the virtual control method is introduced and a convergence result is proven. In particular, the cost functionals are shown to tend to zero when the viscosity coefficient tends to zero. Section 4 is dedicated to 2D numerical results assessing the theoretical analysis given in Sect. 3. These results are obtained by the spectral element method (which is equivalent to p-finite elements). When overlapping domains are considered, entire spectral elements are overlapped. In Sects. 5 and 6 we consider the non overlapping situation; the analysis on several cost functionals is given, and both 2D and 1D numerical results are shown.

2. Overlapping situation

We consider a two-dimensional domain Ω. Remarks concerning the one-dimensional particular case will be made later. We adopt the following notation (see Figs. 1 and 2 for two possible examples): Ω_1 and Ω_2 are two subdomains of Ω such that

$$\bar{\Omega} = \bar{\Omega}_1 \cup \bar{\Omega}_2,\ \Omega_1 \cap \Omega_2 \neq \emptyset, \tag{1}$$

$$\Gamma = \partial\Omega = \Gamma_1 \cup \Gamma_2, \tag{2}$$

$$\partial\Omega_1 = \Gamma_1 \cup S_1,\ \partial\Omega_2 = \Gamma_2 \cup S_2. \tag{3}$$

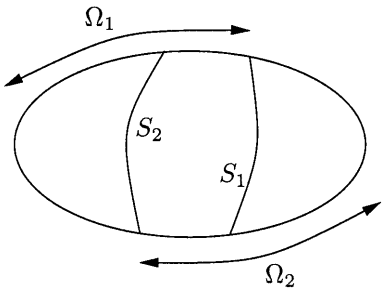

Fig. 1. A decomposition of the domain Ω by two overlapping subdomains

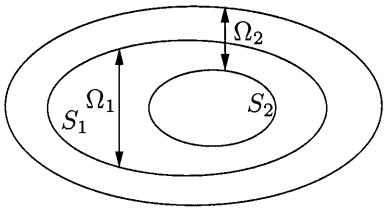

Fig. 2. Another decomposition of Ω, this time by "imbedded" subdomains

Note that $\Gamma_1 \cap \Gamma_2 \neq \emptyset$ in the case of Fig. 1, whereas $\Gamma_1 \cap \Gamma_2 = \emptyset$ in the case of Fig. 2 (indeed, in Fig. 2 $\Gamma_1 = \emptyset$ and $\Gamma_2 = \partial\Omega$).

We define the differential operators

$$L_1 \equiv \mathrm{div}(\mathbf{b}\cdot) + b_0,\ L_2 \equiv -\nu\Delta + \mathrm{div}(\mathbf{b}\cdot) + b_0, \tag{4}$$

where $\nu = const > 0$, $\mathbf{b}$ and b_0 are given data that satisfy $\left(\frac{1}{2}\mathrm{div}\mathbf{b} + b_0\right) \geq \mu_0$ for a suitable constant $\mu_0 > 0$.

The global Dirichlet problem in Ω is

$$\begin{aligned} L_2 u &= f \text{ in } \Omega, \\ u &= g \quad \text{ on } \Gamma, \end{aligned} \tag{5}$$

a problem which admits a unique solution under "reasonable" hypotheses on the data f, g, $\mathbf{b}$ and b_0, hypotheses that there is no need to present here. Our decoupling of problem (5) is based on two steps:

1. the classical domain decomposition where we address the same differential problem (5) in both Ω_1 and Ω_2;
2. the possibility of using in Ω_1 the simplest operator L_1, instead of the global operator L_2, this is what we call heterogeneous domain decomposition (the homogeneous corresponds to using L_2 in Ω_1 as well).

Remark 1 The heterogeneous decomposition is for instance motivated by the presence of boundary layers arising from (5) when ν is small compared to $|\mathbf{b}|$ or $|b_0|$. It is then more natural to take for Ω_2 a strip around Γ and for Ω_1 an inner domain as described in Fig. 2.

Remark 2 All that follows is completely general, i.e. applies to any decomposition $\Omega = \Omega_1 \cup \ldots \cup \Omega_m$ with arbitrary operators.

3. The virtual control method

Let us define

$$\Gamma_{1D} = \{\mathbf{x} |\ \mathbf{x} \in \Gamma_1,\ \mathbf{b}(\mathbf{x}) \cdot \mathbf{n}(\mathbf{x}) < 0\}\,,$$

$$S_{1D} = \{\mathbf{x} |\ \mathbf{x} \in S_1,\ \mathbf{b}(\mathbf{x}) \cdot \mathbf{n}(\mathbf{x}) < 0\}\,,$$

where $\mathbf{n}$ denotes the outward unit normal vector on the boundary at hand.

The heterogeneous decomposition is formulated through two unknown functions λ_1 and λ_2 as follows:

$$\begin{aligned} L_1 u_1 &= f \ \text{ in } \Omega_1, \\ u_1 &= g \ \text{ on } \Gamma_{1D}, \\ u_1 &= \lambda_1 \text{ on } S_{1D}, \end{aligned} \tag{6}$$

$$\begin{aligned} L_2 u_2 &= f \ \text{ in } \Omega_2, \\ u_2 &= g \ \text{ on } \Gamma_2, \\ u_2 &= \lambda_2 \text{ on } S_2, \end{aligned} \tag{7}$$

where λ_1 is the *first virtual control*. In the case where

$$S_{1D} = \emptyset \tag{8}$$

no virtual control is introduced, as there is no need to prescribe any boundary data on S_1 for problem (6). The *second virtual control* is λ_2. The virtual controls λ_1 and λ_2 are chosen so that u_1 and u_2 "adjust" in the best possible way on $\Omega_1 \cap \Omega_2$.

The solution u_1 (respectively, u_2) of (6) (respectively (7)) is a function of λ_1 (resp. λ_2) (with the exception of case (8)), $u_i = u_i(\lambda_i)$.

Remark 3 Although we are focusing here on the Dirichlet boundary conditions, accounting for other boundary conditions (Neumann's or mixed) would not introduce extra difficulties.

To express the "adjustment", in the framework of (virtual) control theory, we introduce the "cost" functional

$$J(\lambda_1, \lambda_2) = \frac{1}{2} \int_{\Omega_1 \cap \Omega_2} (u_1(\lambda_1) - u_2(\lambda_2))^2 \, dx, \tag{9}$$

and consider the minimization problem:

$$\inf_{\lambda_1, \lambda_2} J(\lambda_1, \lambda_2). \tag{10}$$

Remark 4 (The homogeneous decomposition) For the homogeneous decomposition, one keeps L_2 in Ω_1, i.e. one considers u_1 to be given now by

$$\begin{aligned} L_2 u_1 &= f \text{ in } \Omega_1, \\ u_1 &= g \text{ on } \Gamma_1, \\ u_1 &= \lambda_1 \text{ on } S_1, \end{aligned} \tag{11}$$

and we consider again (9), (10).

In that case $\inf_{\lambda_1,\lambda_2} J(\lambda_1,\lambda_2) = 0$, which is achieved by taking λ_i equal to the restriction (trace) on S_i of the space where the solution u of (5) belongs to.

Remark 5 We have not made precise the space where the virtual controls should be chosen. In the heterogeneous decomposition, this is not a simple matter in the infinite dimensional (continuous) case, as we now explain.

Let us consider problem (10). The solution u_1 (resp. u_2) of (6) (resp. (7)) is

$$u_1 = u_1^0 + v_1,\ u_2 = u_2^0 + v_2,$$

where, for $i = 1, 2$ u_i^0 depends on the data f and g whereas v_i depends on λ_i as follows

$$\begin{array}{llll} L_1 u_1^0 = f & \text{in } \Omega_1,\ u_1^0 = g & \text{on } \Gamma_{1D},\ u_1^0 = 0 & \text{on } S_{1D}, \\ L_1 v_1 = 0 & \text{in } \Omega_1,\ v_1 = 0 & \text{on } \Gamma_{1D},\ v_1 = \lambda_1 & \text{on } S_{1D}, \end{array}$$

and analogously

$$\begin{array}{llll} L_2 u_2^0 = f & \text{in } \Omega_2,\ u_2^0 = g & \text{on } \Gamma_2,\ u_2^0 = 0 & \text{on } S_2, \\ L_2 v_2 = 0 & \text{in } \Omega_2,\ v_2 = 0 & \text{on } \Gamma_2,\ v_2 = \lambda_2 & \text{on } S_2. \end{array}$$

Then

$$J(\lambda_1,\lambda_2) = \frac{1}{2} Q(\lambda_1,\lambda_2) + \mathcal{L}(\lambda_1,\lambda_2), \tag{12}$$

where the quadratic functional Q is given by

$$Q(\lambda_1,\lambda_2) = \int_{\Omega_1 \cap \Omega_2} (v_1 - v_2)^2 \, dx, \tag{13}$$

while $\mathcal{L}$ is an affine functional. Consequently, if the functions λ_i are smooth enough, one can define a semi-norm

$$|||\{\lambda_1,\lambda_2\}||| = (Q(\lambda_1,\lambda_2))^{1/2}, \tag{14}$$

on the space of $\{\lambda_1,\lambda_2\}$.

Actually, this is a *norm*. We prove it in the case of Fig. 1. Indeed, if $Q(\lambda_1, \lambda_2) = 0$, then $v_1 = v_2 = v$ in $\Omega_1 \cap \Omega_2$. Therefore, $L_2 v - L_1 v = -\nu \Delta v = 0$ in $\Omega_1 \cap \Omega_2$ and $v = 0$ on $\partial(\overline{\Omega_1 \cap \Omega_2}) \cap \Gamma$.

Moreover, since $L_1 v = 0$ in $\Omega_1 \cap \Omega_2$, taking (formally) this equation to the boundary, one finds

$$(\mathbf{b} \cdot \mathbf{n}) \frac{\partial v}{\partial n} = 0 \text{ on } \partial(\overline{\Omega_1 \cap \Omega_2}) \cap \Gamma. \tag{15}$$

Therefore if there exists $\Sigma \subset \partial(\overline{\Omega_1 \cap \Omega_2}) \cap \Gamma$, with $\mathrm{meas}\Sigma \neq 0$, with

$$\mathbf{b} \cdot \mathbf{n} \neq 0 \text{ on } \Sigma, \tag{16}$$

the Cauchy data of v are zero on $\partial(\overline{\Omega_1 \cap \Omega_2}) \cap \Sigma$, and $\Delta v = 0$ in $\Omega_1 \cap \Omega_2$ so that $v \equiv 0$ in $\Omega_1 \cap \Omega_2$ by the unique continuation theorem. Then $\lambda_1 = 0$ and $\lambda_2 = 0$, thus (14) is a norm.

Different arguments are needed in the case of Fig. 2.

Therefore if all data are smooth enough, and if (16) holds true, $\inf J(\lambda_1, \lambda_2)$ admits a solution in the space of $\{\lambda_1, \lambda_2\}$ obtained by completion for the norm (14).

Remark 6 The abstract space obtained by completion is "very large", but of course this point is irrelevant when using finite dimensional approximations, provided discrete versions of uniqueness theorems hold true.

Indeed, although our numerical results are in full agreement with the theoretical conclusions drawn on the differential problem, the proof of the uniqueness theorem at the finite dimensional level would require separate investigation.

Remark 7 The previous proof can be carried out also in the case of Neumann boundary condition on $\partial(\overline{\Omega_1 \cap \Omega_2}) \cap \Gamma$. On the other hand, the same proof does not apply (in general) when $\mathbf{b} \cdot \mathbf{n} = 0$ on $\partial(\overline{\Omega_1 \cap \Omega_2}) \cap \Gamma$. However, (14) can still be proven to be a norm by ad-hoc argument in some special circumstances (cf. Remark 4.1 below). In any case, we didn't experience any difficulty with our numerical algorithms (cf. Sect. 4.1).

Remark 8 Assume that $S_{1D} = \emptyset$. Then $v_1 = 0$ so that $v_2 = 0$ in $\Omega_1 \cap \Omega_2$. But $L_2 v_2 = 0$ in Ω_2, so that by the unique continuation theorem $v_2 \equiv 0$ in Ω_2, hence $\lambda_2 = 0$ and the same remarks as above apply. See Sect. 4.1 for numerical results about this situation.

Remark 9 In the 1D case let us consider the operators $L_1 u = (bu)_x + b_0 u$, $L_2 u = -\nu u_{xx} + (bu)_x + b_0 u$, where b and b_0 are constant. This case is degenerate, since $\partial(\overline{\Omega_1 \cap \Omega_2}) \cap \Gamma$ does not make sense and the above proof is not valid anymore. If $b < 0$ on S_1, then v_1 is defined as above and

$v_1 = v_2 = v$ in $\Omega_1 \cap \Omega_2$ implies $d^2v_2/dx^2 = 0$ in $\Omega_1 \cap \Omega_2$. Since $L_2 v_2 = 0$ in Ω_2, $d^2v_2/dx^2 = 0$ in $\Omega_1 \cap \Omega_2$ implies that $v_2 = 0$ hence $\lambda_2 = 0$. Then $v_1 = 0$ in $\Omega_1 \cap \Omega_2$ hence $\lambda_1 = 0$.

If $b > 0$ on S_1, there is no virtual control λ_1 again and one finds that $\lambda_1 = 0$. Numerical results for the 1D case are given in Sects. 4.4 and 4.5.

Let us prove now the following result.

Theorem 1 *If we set*

$$\phi(\nu) = \inf_{\lambda_1, \lambda_2} J(\lambda_1, \lambda_2) \tag{17}$$

and if we let $\nu \to 0$*, all other data being fixed, then*

$$\phi(\nu) \to 0 \text{ as } \nu \to 0. \tag{18}$$

Proof Let us denote by u_ν (resp. u_0) the solution of

$$L_2 u_\nu = f \text{ in } \Omega,\ u_\nu = g \text{ on } \Gamma,$$

(resp. $L_1 u_0 = f$ in Ω, $u_0 = g$ on Γ_D). We define

$$\begin{aligned} \lambda_2 &= \text{trace of } u_\nu \text{ on } S_2, \\ \lambda_1 &= \text{trace of } u_0 \text{ on } S_{1D} \end{aligned} \tag{19}$$

(no λ_1 is introduced if $S_{1D} = \emptyset$). Then $u_2 = u_\nu$ in Ω_2, $u_1 = u_0$ on Ω_1 and therefore

$$J(\lambda_1, \lambda_2) = \frac{1}{2} \int_{\Omega_1 \cap \Omega_2} (u_\nu - u_0)^2 dx,$$

Hence (18) follows, since $u_\nu \to u_0$ in $\mathrm{L}^2(\Omega)$ (in particular). □

Numerical evidence for this result is given in Sect. 4 (see Figs. 3, 4, 6, 7 and 8).

4. Numerical experiments for the overlapping case

The approximation of the boundary-value problems in (6) and (7) is done by using conformal spectral elements (see [1,10]), where N denotes the polynomial degree used in each direction of each element. The overlapping region contains entire elements, in general one spectral element along the direction of the overlapping.

In order to minimize the cost functional (9) we use, for convenience, the Principal Axis Method (see [2]), more efficient optimisation methods being used in [6].

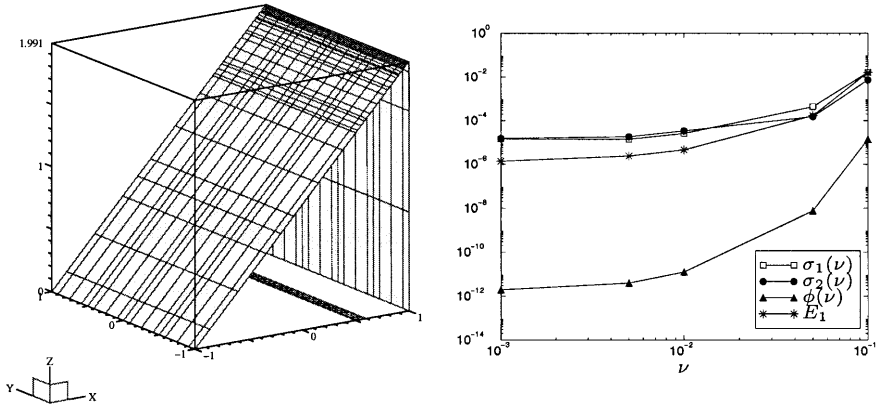

Fig. 3. $S_{1D} = \emptyset$. Test case #1. The overlap is $\Omega_1 \cap \Omega_2 = (.5, .6) \times (-1, 1)$. On the left the spectral elements solution with $\nu = 10^{-3}$ is shown. On the overlapping area we have plotted the arithmetic mean of the two solutions in Ω_1 and Ω_2. On the right picture the maximum interface errors (22) and the function ϕ (17) and the error (23) are shown for different values of the viscosity ν

4.1. 2D case. $S_{1D} = \emptyset$

Test case #1. We have considered the following data:

$$\Omega = (-1, 1)^2,\ \Omega_1 = (-1, .6) \times (-1, 1),\ \Omega_2 = (.5, 1) \times (-1, 1) \tag{20}$$

$$\mathbf{b} = [1, 0]^{\mathrm{t}},\ b_0 = 0,\ f \equiv 1. \tag{21}$$

We have imposed homogeneous Dirichlet conditions on the vertical sides of Ω and null normal derivative on the horizontal sides of Ω. In this case we have $S_{1D} = \emptyset$. Spectral elements with polynomial degree $N = 3$ in both directions x and y are used if $x \leq .99$, while in the strip $[0.99, 1] \times [-1, 1]$ spectral elements are used with $N = 8$ along the x coordinate and $N = 3$ along the y coordinate.

In Fig. 3 we show the numerical solution obtained with viscosity $\nu = 10^{-3}$, the maximum interface error

$$\sigma_i(\nu) = \max_{\mathbf{x} \in S_i} |u_{1,\nu}(\mathbf{x}) - u_{2,\nu}(\mathbf{x})| \tag{22}$$

and the error in H^1-norm with respect to the global elliptic solution, i.e.

$$E_1 = \frac{\|u_J - u\|_{H^1(\Omega)}}{\|u\|_{H^1(\Omega)}}, \tag{23}$$

where u_J and u are the numerical solutions corresponding to problems (10) and (5), respectively. Moreover we assess the conclusion of Theorem 1.

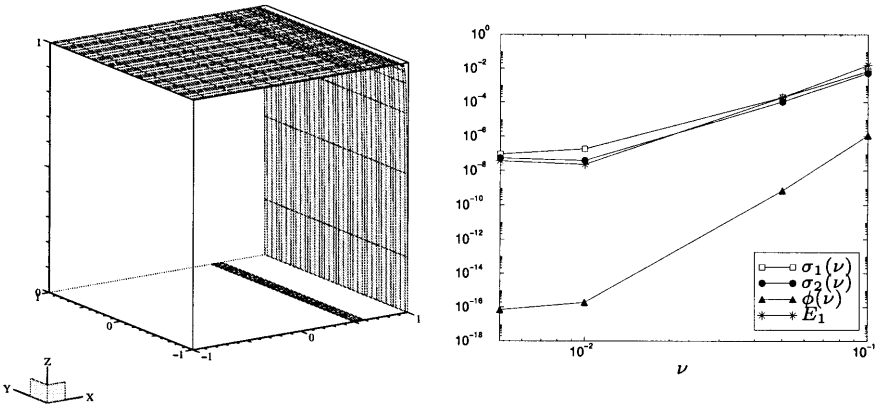

Fig. 4. $S_{1D} = \emptyset$. Test case #2. The overlap is $\Omega_1 \cap \Omega_2 = (.5, .6) \times (-1, 1)$. On the left the spectral elements solution with $\nu = 10^{-2}$ is shown. On the overlapping area we have plotted the arithmetic mean of the two solutions in Ω_1 and Ω_2. On the right picture the maximum interface errors (22), the function ϕ (17) and the error (23) are shown for different values of the viscosity ν

Test case #2. Another test case with $S_{1D} = \emptyset$ is obtained with the same data given in (20)-(21), but now with $f \equiv 0$. We have imposed homogeneous Dirichlet conditions ($g \equiv 0$) on the right vertical side of Ω, $g \equiv 1$ on the left vertical side, and null normal derivative on the horizontal sides. Spectral elements with polynomial degree $N = 4$ are used if $x \leq .9$, while in the strip $[0.9, 1] \times [-1, 1]$ spectral elements are used with $N = 8$ along the x coordinate and $N = 4$ along the y coordinate.

In Fig. 4 the solution obtained with $\nu = 10^{-2}$ is shown, together with the maximum interface errors (22) and the function ϕ (17).

Remark 10 In this test case, $\mathbf{b} \cdot \mathbf{n} = 0$ on $\partial(\overline{\Omega_1 \cap \Omega_2}) \cap \Gamma$ so that the reasoning that was used in Sect. 3, to prove that (14) is a norm, does not apply. However, since $v_1 = v_2 = v$, we have on one hand that $L_1 v_1 = 0$, i.e. $\frac{\partial v_1}{\partial x} = 0$ so that $v = v(y)$. Hence, $L_2 v_2 = 0$ reduces to $-\nu \frac{\partial^2 v}{\partial y^2} = 0$, i.e.

$$v = c_0 + c_1 y, \qquad c_0, c_1 \text{ constants.}$$

But $v = 0$ for $y = \pm 1$ implies $c_0 = c_1 = 0$, hence $v = 0$ and (14) is a norm in this case as well.

Test case #3. We considered the following data:

$$\Omega = (-1, 1)^2,\ \Omega_1 = (-1, 0) \times (-1, 0.75),$$
$$\Omega_2 = \Omega \setminus (-1, -0.25) \times (-1, 0.5),$$
$$\mathbf{b} = \frac{1}{2}[(1 - x^2)(1 + y), -x(4 - (1 + y)^2)]^{\mathrm{t}},\ b_0 = 10^{-4},\ f \equiv 0.$$

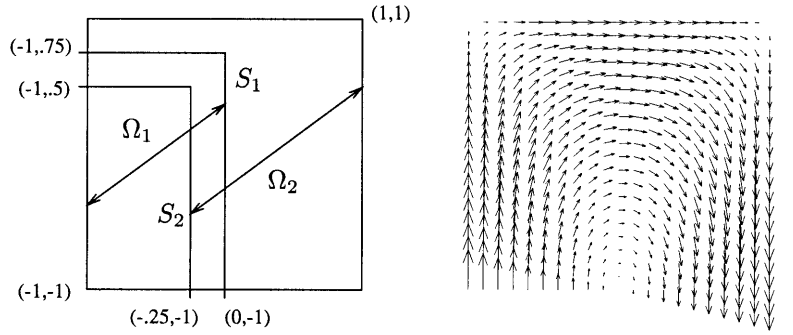

Fig. 5. On the left the domain decomposition used for the test case #3, on the right the vector field $\mathbf{b}$ on the computational domain Ω

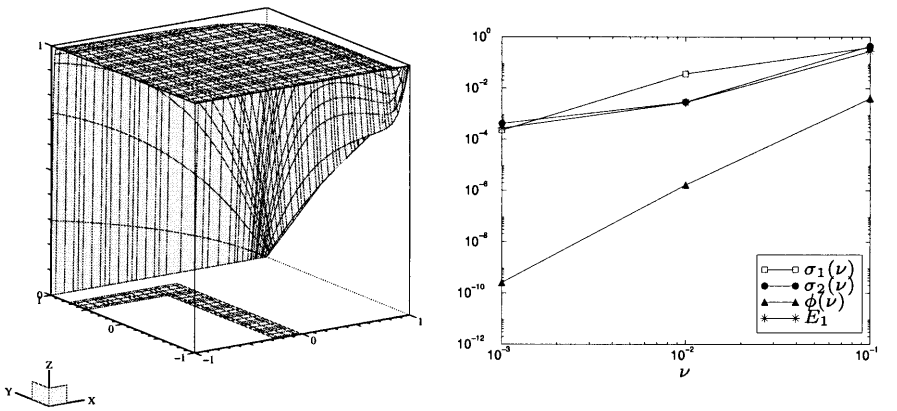

Fig. 6. $S_{1D} = \emptyset$. Test case #3. On the left the numerical solution with $\nu = 10^{-3}$ is shown. On the right picture the maximum interface errors (22), the function ϕ (17) and the error (23) are shown for different values of the viscosity ν

We have imposed the Dirichlet condition $g(x, y) = (1 - y)/2$ on the horizontal sides and on the right vertical side of Ω, while null normal derivative was prescribed on the left vertical side.

Spectral elements of degree $N = 4$ are used and the mesh is finer near to both upper horizontal side and right vertical side. In Fig. 5 the domain decomposition and the vector field $\mathbf{b}$ are plotted. In Fig. 6 the numerical solution computed with $\nu = 10^{-2}$ is shown.

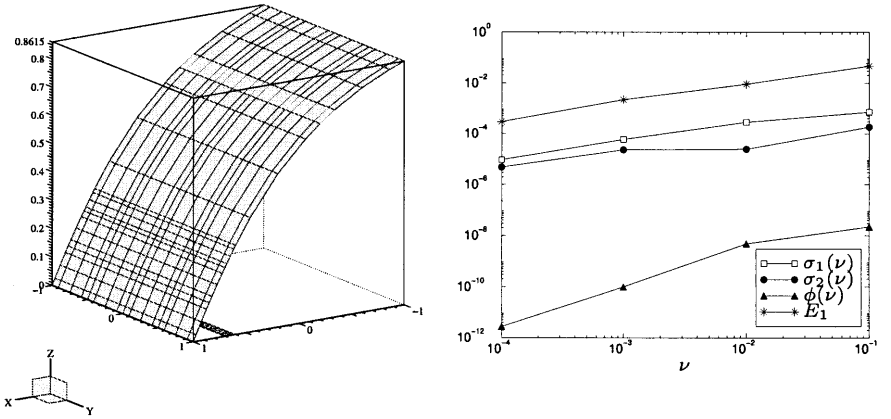

Fig. 7. $S_{1D} = S_1$. Test case #4. The overlap is $\Omega_1 \cap \Omega_2 = (.6, .7) \times (-1, 1)$. On the left the spectral elements solution with $\nu = 10^{-1}$ and with polynomial degree $N = 4$ is shown. On the overlapping area we have plotted the arithmetic mean of the two solutions u_1 and u_2. On the right picture the maximum interface errors (22), the function ϕ (17) and the error (23) are shown for different values of the viscosity ν

4.2. 2D case. $S_{1D} = S_1$

Test case #4. We have considered the following data:

(24) $\Omega = (-1, 1)^2,\ \Omega_1 = (-1, .7) \times (-1, 1),\ \Omega_2 = (.6, 1) \times (-1, 1)$

(25) $\mathbf{b} = [-1, 0]^{\mathrm{t}},\ b_0 = 1,\ f \equiv 1.$

We have imposed homogeneous Dirichlet conditions on the right vertical side of Ω and null normal derivative on the horizontal sides of Ω. In Fig. 7 we show the numerical solution obtained with viscosity $\nu = 10^{-1}$, the behaviour of the maximum interface errors (22) and the function ϕ (17) versus the viscosity ν.

4.3. 2D case. $S_{1D} \neq \emptyset$, $S_{1D} \subsetneq S_1$

Test case #5. We have considered the following data:

(26) $\Omega = (-1, 1)^2,\ \Omega_1 = (-1, .8) \times (-1, 1),\ \Omega_2 = (.7, 1) \times (-1, 1),$

(27) $\mathbf{b} = [y, 0]^{\mathrm{t}},\ b_0 = 1,\ f \equiv 1.$

We have imposed homogeneous Dirichlet conditions on the right vertical side of Ω, $g \equiv 1$ on $\{-1\} \times [0, 1]$ and null normal derivative on the horizontal sides of Ω and on $\{-1\} \times (-1, 0)$. In this case we have $S_{1D} = \{.8\} \times (-1, 0)$. Along the y coordinate the mesh is uniform, while along the x coordinate the mesh is finer near the boundary layer. In Fig. 8 we show the numerical solution obtained with viscosity $\nu = 10^{-1}$, the maximum interface errors (22) and we assess the thesis of Theorem 1.

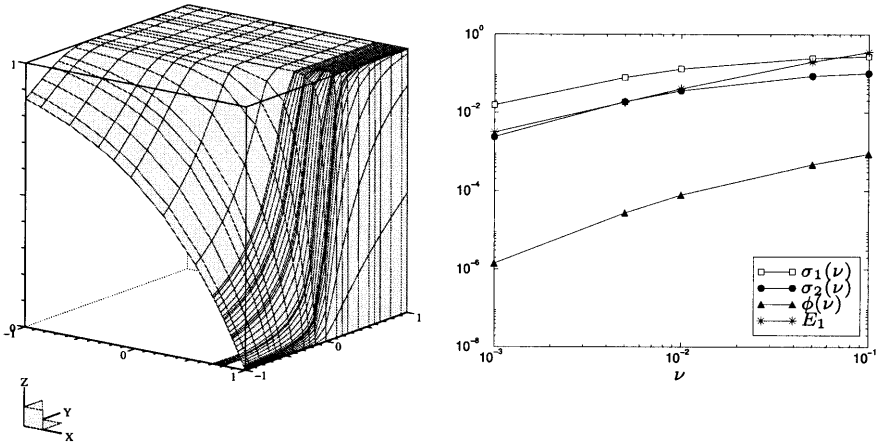

Fig. 8. Test case #5. $S_{1D} = \{x = .8,\ -1 < y < 0\}, \nu = 10^{-3}$. The overlap is $\Omega_1 \cap \Omega_2 = (.7, .8) \times (-1, 1)$. On the overlapping area we have plotted the arithmetic mean of the two solutions in Ω_1 and Ω_2. On the right picture the maximum interface errors (22), the function ϕ (17) and the error (23) are shown for different values of the viscosity ν

4.4. 1D case. $S_{1D} = \emptyset$

Test case #6. We have considered the following data:

$$\Omega = (0,1),\ \Omega_1 = (0, 0.7),\ \Omega_2 = (0.6, 1), \tag{28}$$

$$b_1 = 1,\ b_0 = 0,\ f \equiv 1,\ \ g \equiv 0, \tag{29}$$

hence $S_{1D} = \emptyset$.

In Fig. 9 the solution of (10) is compared with the global elliptic solution of (5). Both solutions are computed with spectral elements of diameter $H = 0.5$ and degree $N = 5$.

Remark 11 We have computed the solution with various N (spectral polynomial degree) and H (elements diameter) and we have observed that the difference between the solution and the global elliptic solution does not depend on N nor on H, but only on the viscosity coefficient. In particular, this difference tends to zero when $\nu \to 0$.

4.5. 1D case. $S_{1D} = S_1$

Test case #7. We have considered the following data:

$$\Omega = (0,1),\ \Omega_1 = (0, 0.7),\ \Omega_2 = (0.6, 1). \tag{30}$$

$$b_1 = -1,\ b_0 = 1,\ f \equiv 1,\ \ g \equiv 0, \tag{31}$$

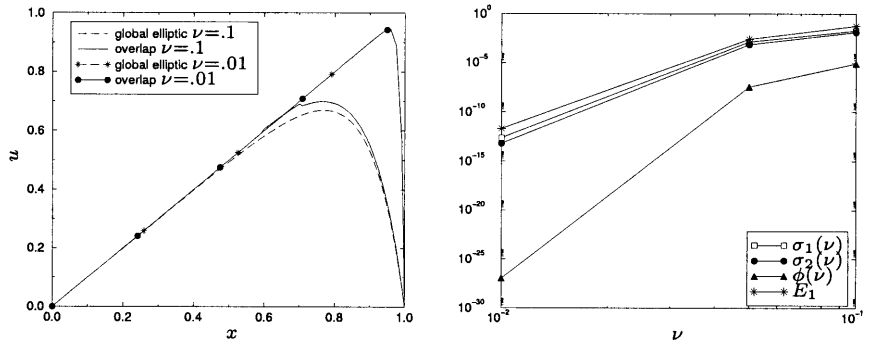

Fig. 9. Test case #6. Coupling with overlapping with $\nu = 10^{-1}$ and $\nu = 10^{-2}$. The overlapping is $\Omega_1 \cap \Omega_2 = (0.6, 0.7)$. On the overlapping area we have plotted the arithmetic mean of the two solutions in Ω_1 and Ω_2. On the right picture the maximum interface errors (22), the function ϕ (17) and the error (23) are shown for different values of the viscosity ν

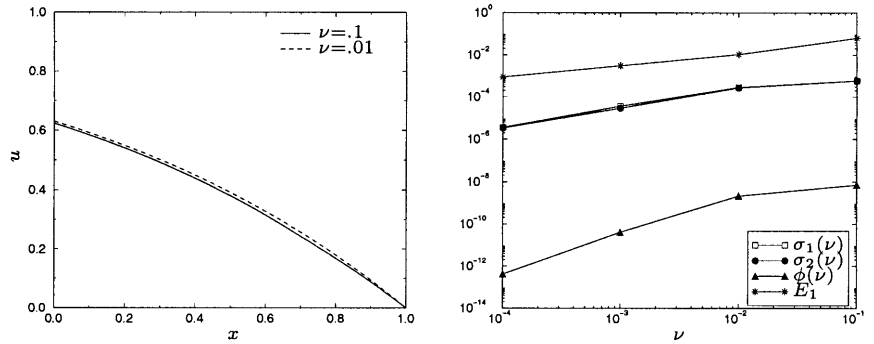

Fig. 10. Test case #7. Coupling with overlapping with $\nu = 10^{-1}$ and $\nu = 10^{-2}$. The overlapping is $\Omega_1 \cap \Omega_2 = (0.6, 0.7)$. On the overlapping area we have plotted the arithmetic mean of the two solutions in Ω_1 and Ω_2. On the right picture the maximum interface errors (22), the function ϕ (17) and the error (23) are shown for different values of the viscosity ν

We have that $S_1 = S_{1D}$.

In Fig. 10 we report the solution of (10) for $\nu = 10^{-1}$ and $\nu = 10^{-2}$, computed with spectral elements of diameter $H = 0.5$ and degree $N = 4$. Moreover the numerical behaviour of $\phi(\nu)$ (17) and the maximum interface errors (22) are shown.

Remark 12 In all cases considered above, the method provides the expected (correct) results in the sense that $\phi(\nu) \to 0$ as $\nu \to 0$.

5. The non overlapping situation

We consider now the situation represented in Fig. 11 which refers to the case where Ω is partitioned into two disjoint subdomains whose interface is S.

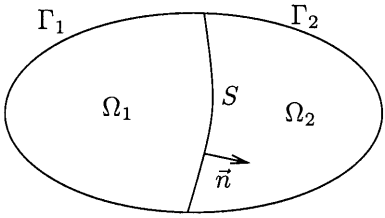

Fig. 11. A disjoint partition of Ω

We define u_1 in Ω_1 by

$$\begin{array}{ll} L_1 u_1 = f \text{ in } \Omega_1, \\ u_1 = g \quad \text{on } \Gamma_{1D}, \\ u_1 = \lambda_1 \quad \text{on } S_D, \end{array} \tag{32}$$

where $S_D = \{\mathbf{x} \in S |\ \mathbf{b}(\mathbf{x}) \cdot \mathbf{n}(\mathbf{x}) < 0\}$, $\mathbf{n}$ being the unit normal vector on S directed from Ω_1 to Ω_2.

Remark 13 If $S_D = \emptyset$, there is no condition on S_D and no virtual control is attached to u_1. This situation in somewhat paradoxical, however, one should notice that in this case S is an outflow boundary for the advection problem (32).

We then define u_2 in Ω_2 by

$$\begin{array}{ll} L_2 u_2 = f \text{ in } \Omega_2, \\ u_2 = g \quad \text{on } \Gamma_2, \\ u_2 = \lambda_2 \quad \text{on } S. \end{array} \tag{33}$$

Remark 14 The situation described above corresponds to the heterogeneous case. If we take $L_1 = L_2$ in (32) (and $\Gamma_{1D} = \Gamma_1$, $S_D = S$), we are dealing with the homogeneous case.

We want now to choose $\lambda = \{\lambda_1, \lambda_2\}$ so that u_1 and u_2 "adjust" in the best possible way on S. Contrary to the overlapping case where there is "reasonable uniqueness"of the adjustment functional, several cases have to be considered in the non overlapping case. The natural functionals to introduce are the following ones (their properties are analyzed below):

$$J_1(\lambda_1, \lambda_2) = \frac{1}{2} \int_S (u_1 - u_2)^2 ds, \tag{34}$$

where $u_i = u_i(\lambda_i)$ is the solution of (32) or (33);

$$J_2(\lambda_1, \lambda_2) = \frac{1}{2} \int_S (u_1 - u_2)^2 ds + \frac{1}{2} \int_S (\phi_1 - \phi_2)^2 ds, \tag{35}$$

where

$$\phi_1 = -\mathbf{b}\cdot\mathbf{n}u_1 \text{ on } S, \tag{36}$$

$$\phi_2 = \nu\mathbf{n}\cdot\nabla u_2 - \mathbf{b}\cdot\mathbf{n}u_2 \text{ on } S; \tag{37}$$

finally,

$$J_3(\lambda_1,\lambda_2) = \frac{1}{2}\int_S (\phi_1-\phi_2)^2 ds. \tag{38}$$

We want now to analyze the respective advantages of (34), (35) and (36). We proceed as in Sect. 2, and introduce v_1 and v_2 by

$$\begin{aligned} &L_1 v_1 = 0 \text{ in } \Omega_1,\\ &v_1 = 0 \quad \text{on } \Gamma_{1D},\\ &v_1 = \lambda_1 \quad \text{on } S_D; \end{aligned} \tag{39}$$

$$\begin{aligned} &L_2 v_2 = 0 \text{ in } \Omega_2,\\ &v_2 = 0 \quad \text{on } \Gamma_2,\\ &v_2 = \lambda_2 \quad \text{on } S. \end{aligned} \tag{40}$$

We note that

(41) if $S_D = \emptyset$ then $v_1 = 0$ and no λ_1 is introduced.

Then

$$J_i(\lambda) = \frac{1}{2}Q_i(\lambda) + \mathcal{L}_i(\lambda),\ \ i = 1,2,3, \qquad \lambda = \{\lambda_1,\lambda_2\},$$

where $\mathcal{L}_i$ is an affine functional of λ, while

$$Q_1(\lambda) = \int_S (v_1-v_2)^2 ds, \tag{42}$$

$$Q_2(\lambda) = \int_S (v_1-v_2)^2 ds + \int_S (\phi_1-\phi_2)^2 ds, \tag{43}$$

$$Q_3(\lambda) = \int_S (\phi_1-\phi_2)^2 ds, \tag{44}$$

where ϕ_1 and ϕ_2 are defined in (36) with u_i replaced by v_i.

There will be *existence* of λ achieving $\inf J_i(\lambda)$, possibly in a very large "abstract" space, and if all data are smooth, provided that

(45) $(Q_i(\lambda))^{1/2}$ is a norm on the space of λ

where λ is smooth enough. Then one introduces the completion of the λ's for the above norm and it is in this space that the $\inf J_i$ is achieved. Of course all these spaces reduce to finite dimensional spaces for the numerical approximations introduced hereafter, but it is essential that Q_i be a norm.

Let us examine now the three cases.

The expression $Q_1(\lambda)^{1/2}$.

If $S_D = \emptyset$, (41) then $v_1 = 0$ so that if $Q_1(\lambda) = 0$ then $v_2 = 0$ on S, i.e. $\lambda_2 = 0$. Therefore,

$$\text{if } S_D = \emptyset,\ Q_1(\lambda)^{1/2} \text{ is a norm} \tag{46}$$

and we can expect this functional to lead to interesting numerical results.

If $S_D \neq \emptyset$, then $Q_1(\lambda)^{1/2}$ is not a norm and the numerical approximation are of dubious value. This will be confirmed by the numerical results (cf. Fig. 14, 15).

The expression $Q_2(\lambda)^{1/2}$.

We assume that $S_D \neq \emptyset$, since otherwise, $Q_1(\lambda)^{1/2}$ is already a norm, so a fortiori $Q_2(\lambda)^{1/2}$ is a norm. If $Q_2(\lambda) = 0$ then both $v_1 = v_2$ and $\phi_1 = \phi_2$ on S. Therefore, $\mathbf{n} \cdot \nabla v_2 = 0$ on S (notice that $\phi_1 - \phi_2 = -\nu \mathbf{n} \cdot \nabla v_2$). But this boundary condition used in (40) shows that $v_2 \equiv 0$ in Ω_2, so that $\lambda_2 = 0$. Then, $v_1 = 0$ on S, so that $\lambda_1 = 0$.

Thus, the expression $Q_2(\lambda)^{1/2}$ *is a norm. We can therefore expect the minimization of* $J_2(\lambda)$ *to lead always to reasonably good results as our numerical tests will confirm.*

The expression $Q_3(\lambda)^{1/2}$.

We have

$$\text{if } S_D = \emptyset, \quad Q_3(\lambda)^{1/2} \text{ is a norm.} \tag{47}$$

Indeed, in that case, $v_1 = 0$ and $Q_3(\lambda) = 0$ implies that $\phi_1 = \phi_2$ which thus reduces to $\phi_2 = 0$. This boundary condition, together with (40), implies that $\lambda_2 = 0$ hence (47) follows.

If $S_D \neq \emptyset$, it seems dubious that $Q_3(\lambda)^{1/2}$ is a norm (in fact there are examples where it is not a norm, cf. Remark 16 below), so that the use of $J_3(\lambda)$ is not recommended.

Remark 15 The heterogeneous coupling for the advection-diffusion problem (5) proposed in [4] reads as follows (see also [12], pag. 289):

$$\begin{aligned} L_1 u_1 &= f \quad \text{in } \Omega_1, \\ L_2 u_2 &= f \quad \text{in } \Omega_2, \\ u_i &= g \quad \text{on } \Gamma_i,\ i = 1, 2, \\ u_1 &= u_2 \text{ on } S_D, \\ \phi_1 &= \phi_2 \text{ on } S. \end{aligned} \tag{48}$$

This coupled system is obtained by a perturbation analysis as the limit of the original problem (5) when the viscous coefficient ν is going to zero in Ω_1.

The corresponding solution will be referred to as the *heterogeneous solution.*

Remark 16 There is a more straightforward (but less systematic) way of deriving a priori properties of J_1, J_2, J_3.

Let us begin with J_1, and let us assume first that $S_D \neq \emptyset$. Then, given λ_1 (reasonably) smooth on S_D, (32) defines a function u_1 in Ω_1. Then one can define u_2 by (33) where λ_2 is equal to the trace of u_1 on S. With this choice, $J_1(\lambda_1, \lambda_2) = 0$ and this can be achieved in *infinitely many ways*. As observed before, J_1 is not going to be a "good " functional, *except* if $S_D = \emptyset$. In that case u_1 is uniquely defined (no λ_1 is introduced) and there is a *unique* way to achieve $J_1 = 0$.

If we consider now J_3, the same comments can be applied. If $S_D \neq \emptyset$, one starts with an arbitrary (smooth) function λ_1 and one defines u_2 as the solution of $L_2 u_2 = f$ in Ω_2, $u_2 = g$ on Γ_2 and ϕ_2 (given by (37)) $= \nu \mathbf{n} \cdot \nabla u_1 - \mathbf{b} \cdot \mathbf{n} u_1$ on S. Then $J_3 = 0$ and this can be achieved in *infinitely many ways*, except if $S_D = \emptyset$ in which case there is uniqueness.

Similar arguments do not apply to J_2 as defined in (35). But if we replace J_2 by its variant J_2' (cf. (53) hereafter) then the problem inf J_2' admits a unique solution which *coincides* with the heterogeneous solution introduced in Remark 15 above.

6. Numerical experiments for the non overlapping case

6.1. 2D case. $S_D = \emptyset$

Test case #1 without overlapping. We have considered the data (21), with

$$\Omega = (-1,1)^2,\ \Omega_1 = (-1,.6) \times (-1,1),\ \Omega_2 = (.6,1) \times (-1,1). \tag{49}$$

In this case we have $S_D = \emptyset$. We have imposed homogeneous Dirichlet conditions on the vertical sides of Ω and null normal derivative on the horizontal sides of Ω.

In Fig. 12 we show the numerical solution obtained by minimizing J_1, J_2 and J_3, and the solution of (48) when $\nu = 5 \cdot 10^{-2}$.

The 3 functionals give satisfying results (see Fig. 12).

We denote by u_{J_i} the solutions of $\inf J_i$, for $i = 1, 2, 3$ respectively and by u_{he} the heterogeneous solution of (48).

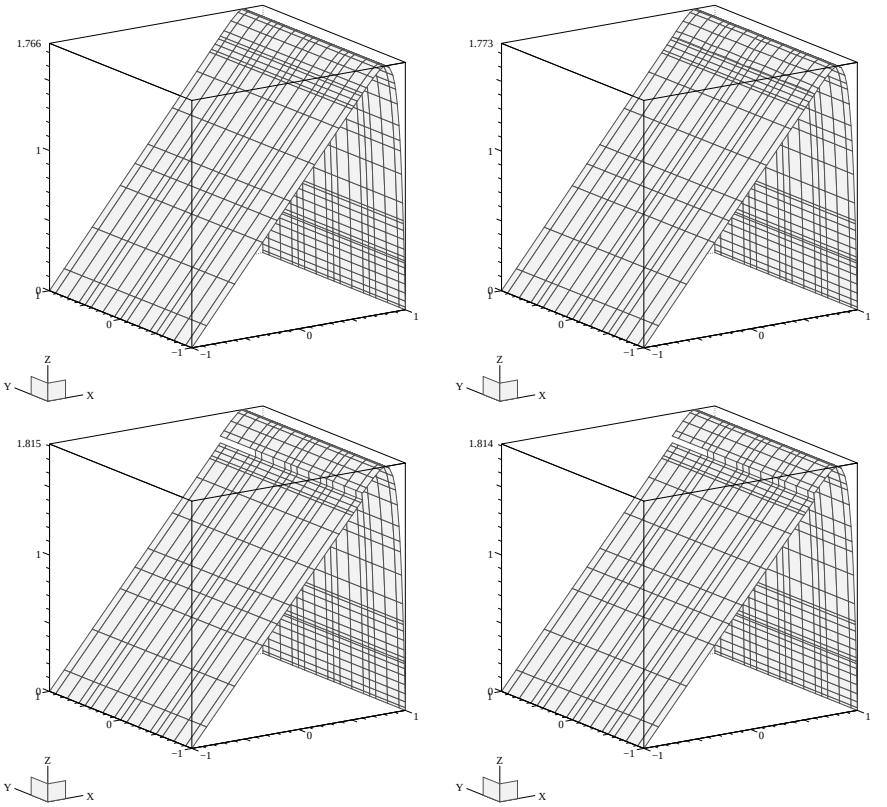

Fig. 12. Test case #1 without overlapping. $S_D = \emptyset$. The solution of $\inf J_1$ (top left), the solution of $\inf J_2$ (top right), the solution of $\inf J_3$ (bottom left) and the heterogeneous solution (48) (bottom right)

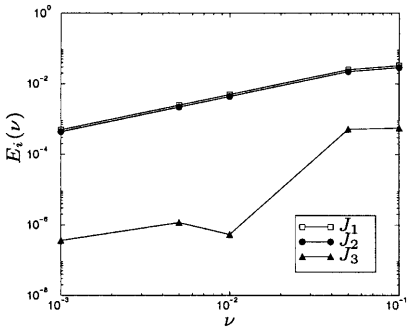

Fig. 13. Test case #1 without overlapping. The quantities $E_i(\nu)$ (50) versus the viscosity ν. We have $S_D = \emptyset$

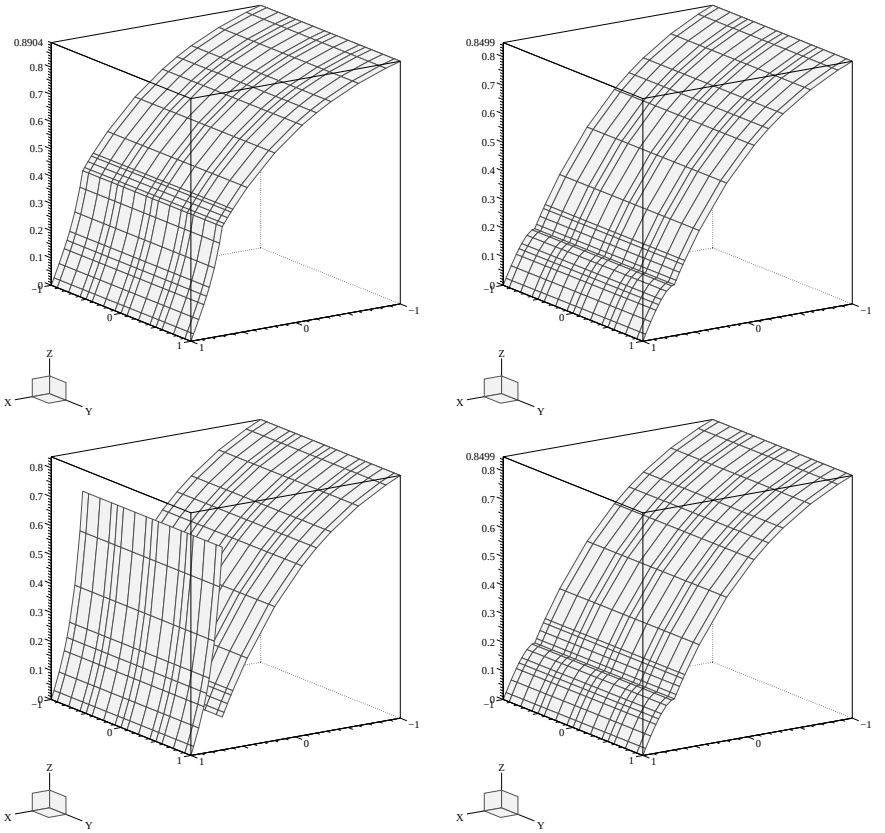

Fig. 14. Test case #4 without overlapping. $S = S_D$. The solution of $\min J_1$ (top left), the solution of $\min J_2$ (top right), the solution of $\min J_3$ (bottom left) and the heterogeneous solution (bottom right). A non uniform mesh with polynomial degree $N = 4$ is considered. Note that the x-axis has been reversed in these pictures

In Fig. 13 we show the quantities:

$$E_i(\nu) = \left(\sum_{j=1}^{2} \frac{\|u_{J_i} - u_{he}\|^2_{H^1(\Omega_j)}}{\|u_{he}\|^2_{H^1(\Omega_j)}} \right)^{1/2} . \tag{50}$$

6.2. 2D case. $S_D = S$

Test case #4 without overlapping. We have considered the data (25) with

$$\Omega = (-1,1)^2,\ \Omega_1 = (-1,.7) \times (-1,1),\ \Omega_2 = (.7,1) \times (-1,1). \tag{51}$$

In this case we have $S_D = S$.

We have imposed homogeneous Dirichlet conditions on the right vertical side of Ω and null normal derivative on the horizontal sides of Ω. In Fig. 14 we show the numerical solution obtained by minimizing J_1, J_3 and J_2, and the heterogeneous solution (48) (the last two solutions do coincide) for $\nu = 10^{-1}$. The solutions obtained by minimizing both J_1 and J_3 depend strongly on the initial guess. The numerical results of Fig. 14 refer to $\lambda_1 = .2$ and $\lambda_2 = .8$.

We have computed the error $E_2(\nu)$ (see (50)) for $\nu = 10^{-1}, 10^{-2}, 10^{-3}$. In all the cases we have obtained $E_2(\nu) \simeq 10^{-13}$.

6.3. 2D case. $\emptyset \neq S_D \subset S$

Test case #5 without overlapping. We have considered the data (27) with

$$\Omega = (-1,1)^2,\ \Omega_1 = (-1,.8)\times(-1,1),\ \Omega_2 = (.8,1)\times(-1,1). \tag{52}$$

In this case we have $S_D = \{.8\}\times(-1,0)$.

We have imposed homogeneous Dirichlet conditions on the right vertical side of Ω, $g \equiv 1$ on $\{-1\}\times[0,1]$ and null normal derivative on the horizontal sides of Ω and on $\{-1\}\times(-1,0)$.

We define a variant of the cost functional J_2 (35) as follows:

$$J_2'(\lambda_1,\lambda_2) = \frac{1}{2}\int_{S_D}(u_1-u_2)^2 ds + \frac{1}{2}\int_S (\phi_1-\phi_2)^2 ds. \tag{53}$$

The associated quadratic functional is

$$Q_2'(\lambda) = \int_{S_D}(v_1-v_2)^2 ds + \int_S (\phi_1-\phi_2)^2 ds \tag{54}$$

where v_1 and v_2 are the solutions of (39) and (40). It is easy to see that $[Q_2'(\lambda)]^{1/2}$ is a norm. In fact, as we have already pointed out in Remark 16, the infimum of J_2' is achieved for the heterogeneous solution (48).

In Fig. 15 we show the numerical solution obtained by minimizing J_1, J_2, J_3, J_2' and the heterogeneous solution (48) for $\nu = 10^{-2}$. We note that the solution obtained by minimizing J_2' and the heterogeneous solution (48) coincide (in agreement with our general remarks). Obviously, the algorithms used here and those used in [12] are totally different, so that we obtain a further validation of our analysis.

6.4. 1D numerical results without overlapping

We note that, for 1D problems, when $\mathbf{b}\cdot\mathbf{n} = b_1 > 0$ we have $S_D = \emptyset$. In this case the interface conditions in (48) ensure the continuity of the flux solely,

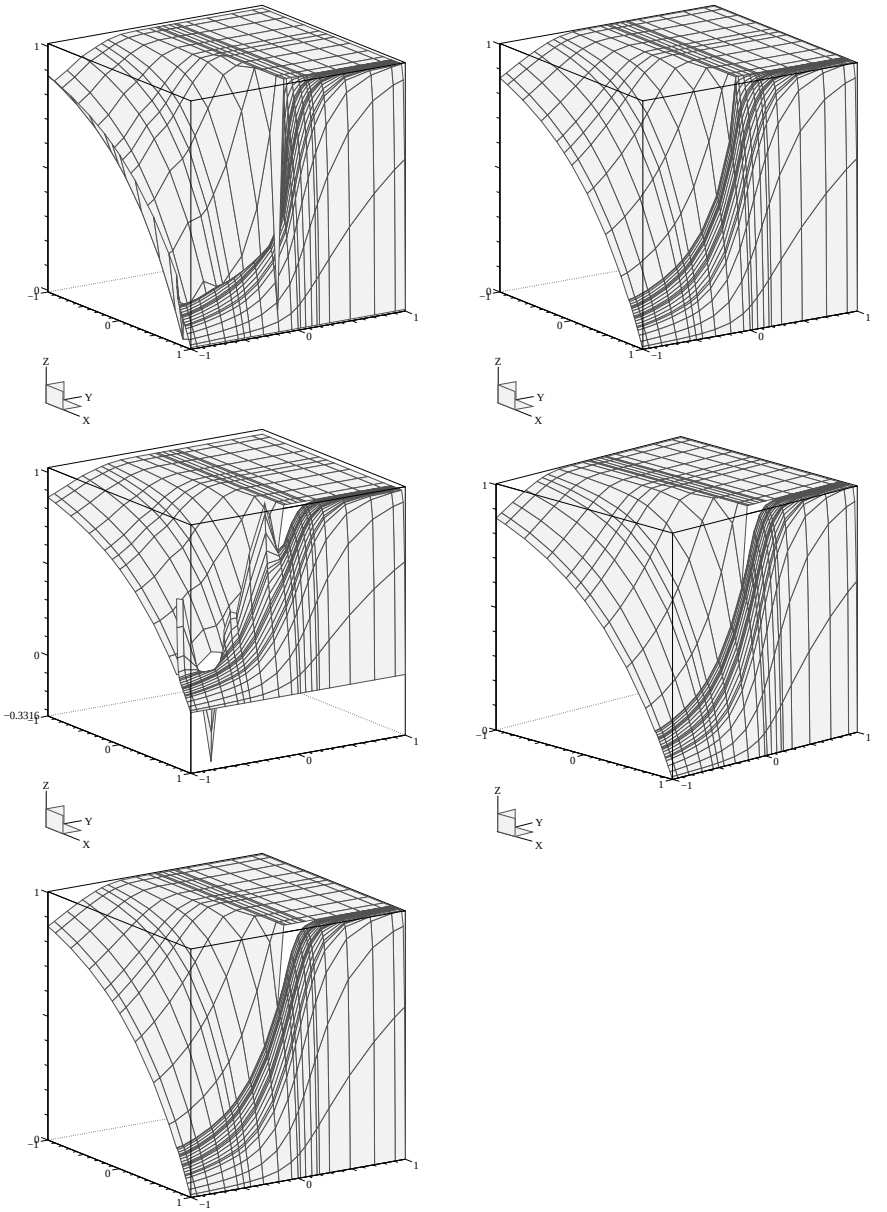

Fig. 15. Test case #5 without overlapping. The sign of $\mathbf{b} \cdot \mathbf{n}$ changes along $S = \{x = .8,\ -1 \leq y \leq 1\}$. The solution corresponding to the minimization of $\min J_1$ (top left), the solution corresponding to the minimization of $\min J_2$ (top right), the solution corresponding to the minimization of $\min J_3$ (medium left), the solution corresponding to the minimization of $\min J_2'$ (medium right) and the heterogeneous solution (48) (bottom left). A non uniform mesh with polynomial degree $N = 5$ is considered

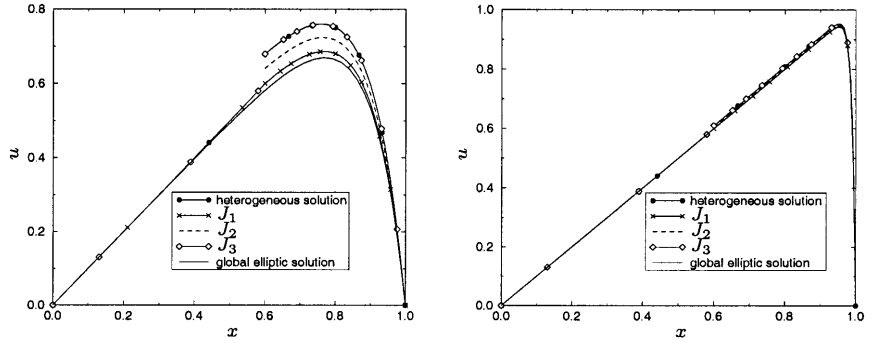

Fig. 16. Test case #6 without overlapping. $S_D = \emptyset$. The viscosity is $\nu = 10^{-1}$ (left) and $\nu = 10^{-2}$ (right). In Ω_1 the solutions computed by minimizing J_1, J_2 and J_3 coincide and the jump across the interface is independent of N and H

i.e. $\phi_2 = \phi_1$ on S. Therefore, the natural candidate for the minimization problem is the functional J_3.

Otherwise, when $\mathbf{b} \cdot \mathbf{n} = b_1 < 0$ we have $S = S_D$. In this case the interface conditions in (48) ensure the continuity of both the solution ($u_1 = u_2$) and the fluxes ($\phi_2 = \phi_1$) on S. It follows that the natural candidate for the minimization problem is the functional J_2.

Test case #6 without overlapping. We have considered the data (29) with

$$\Omega = (0,1),\ \Omega_1 = (0,0.6),\ \Omega_2 = (0.6,1). \tag{55}$$

In Fig. 16 we show the numerical results for $\nu = 10^{-1}$ and $\nu = 10^{-2}$. The multidomain solutions have been computed with one spectral element of degree $N = 6$ in $\Omega_1 = (0, 0.6)$ and six spectral elements of degree $N = 6$ in $\Omega_2 = (0.6, 1)$, while the global elliptic solution has been computed with one spectral element of degree $N = 50$.

Remark 17 When $S_D = \emptyset$, if we assess the quality of the heterogeneous solution by measuring the jump of the solution across the interface $[u]_{|S} = u_{2|S} - u_{1|S}$, we conclude that minimizing J_1 is better than minimizing J_2 and J_3 (see Fig. 16 and Table 1). Otherwise, if we measure the jump of the flux across the interface $[\phi]_{|S} = \phi_{2|S} - \phi_{1|S}$, we conclude that minimizing J_3 is better than minimizing J_1 and J_2 (see Fig. 16 and Table 1).

From Fig. 16 we observe that the solution obtained by minimizing J_3 and the heterogeneous solution (48) coincide, as previously pointed out.

Test case #7 without overlapping. Finally we have considered the data (31) with

$$\Omega = (0,1),\ \Omega_1 = (0,0.6),\ \Omega_2 = (0.6,1). \tag{56}$$

Table 1. Test case #6 without overlapping. 1D case. $S_D = \emptyset$. The jump of the solution and of the flux on the interface, relative to the numerical solutions of Fig. 16. $\epsilon_M \simeq 2.2204e-16$ denotes the floating point machine accuracy

$\nu = 10^{-1}$	$[u]$	$[\phi]$
$\min J_1$	ϵ_M	8.1342e-2
$\min J_2$	4.0664e-2	3.9919e-2
$\min J_3$	7.9852e-2	ϵ_M
global ell.	0.0000e+0	0.0000e+0
heterog.	7.9852e-2	ϵ_M

$\nu = 10^{-2}$	$[u]$	$[\phi]$
$\min J_1$	ϵ_M	1.0000e-2
$\min J_2$	5.0000e-3	4.9999e-3
$\min J_3$	1.0000e-2	ϵ_M
global ell.	0.0000e+0	0.0000e+0
heterog.	1.0000e-2	ϵ_M

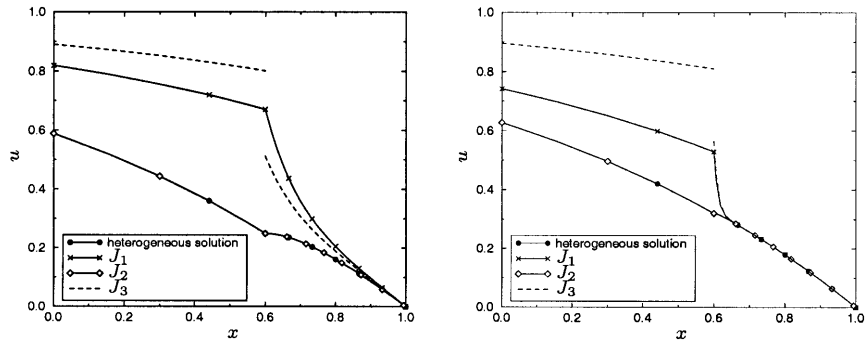

Fig. 17. Test case #7 without overlapping. $S_D = S$. The viscosity is $\nu = .1$ (left) and $\nu = .01$ (right), The discretization is: 1 spectral element of degree $N = 6$ in $\Omega_1 = (0, 0.6)$ and 6 spectral elements of degree $N = 6$ in $\Omega_2 = (0.6, 1)$. The initial guess is $\lambda^0 = [.5, .7]$

The numerical solutions for $\nu = 10^{-1}$ and $\nu = 10^{-2}$ are shown in Fig. 17. We observe that those solutions obtained by minimizing J_1 and J_3 depend on the initial guess λ^0 and are not reliable.

We have computed the error $E_2(\nu)$ (see (50)) for $\nu = 10^{-1}$, 10^{-2}, 10^{-3}. In all the cases we have obtained $E_2(\nu) \simeq 10^{-13}$.

References

1. C. Bernardi, Y. Maday: Approximations Spectrales de Problèmes aux Limites Elliptiques. Paris: Springer, 1992
2. R.P. Brent: Algorithms for minimization without derivatives. Prentice-Hall Series in Automatic Computation. Prentice-Hall, Inc., Englewood Cliffs, NY, 1973
3. T.F. Chan, T.P. Mathew: Domain decomposition algorithms. In Acta Numerica, pp. 61–143. Cambridge Univ. Press, 1994
4. F. Gastaldi, A. Quarteroni: On the coupling of hyperbolic and parabolic systems: analytical and numerical approach. Appl. Numer. Math. **6**, (1) 3–31 (1989)
5. F. Gastaldi, A. Quarteroni, G. Sacchi Landriani: On the coupling of two dimensional hyperbolic and elliptic equations: analytical and numerical approach. In J.Périeaux T.F.Chan, R.Glowinski, O.B.Widlund (Eds.) Third International Symposium on Do-

main Decomposition Methods for Partial Differential Equations, pp. 22–63. SIAM. Philadelphia, 1990
6. P. Gervasio, J.L. Lions, A. Quarteroni: Heterogeneous Coupling by Virtual Control Methods. DD13 Porceedings, in preparation, 2000
7. J.L. Lions, O. Pironneau: Algorithmes parallèles pour la solution de problèmes aux limites. C. R. Acad. Sci. Paris Sér. I Math. t. **327**, 947–952 (1998)
8. J.L. Lions, O. Pironneau: Sur le contrôle parallèle des systèmes distribués. C. R. Acad. Sci. Paris Sér. I Math. t. **327**, 993–998 (1998)
9. J.L. Lions, O. Pironneau: Domain decomposition methods for CAD. C. R. Acad. Sci. Paris Sér. I Math., t. **328**, 73–80 (1999)
10. Y. Maday, A.T. Patera: Spectral element methods for the incompressible Navier-Stokes equations. In State-of-the-Art Surveys on Computational Mechanics. A.K. Noor, J.T. Oden, 1989
11. A. Quarteroni, F. Pasquarelli, A. Valli: Heterogeneous domain decomposition: principles, algorithms, applications. In D.E. Keyes, T.F.Chan, G.Meurant, J.S. Scroggs, R.G. Voigt (Eds.) Fifth International Symposium on Domain Decomposition Methods for Partial Differential Equations, pp. 129–150, SIAM. Philadelphia, 1992
12. A. Quarteroni, A. Valli: Domain Decomposition Methods for Partial Differential Equations. Oxford Science Publications, 1999
13. B.F. Smith, P.E. Bjørstad, W.D. Gropp: Domain Decomposition. Parallel Multilevel Methods for Elliptic Partial Differential Equations. Cambridge: Cambridge, University Press, 1996